Romanian Academy "Ilie Murgulescu"
Institute of Physical Chemistry

THESIS SUMMARY

DESIGN, SYNTHESIS, CHARACTERIZATION AND TESTING OF NANOSTRUCTURED OXIDE MATERIALS FOR SENSOR AND PIEZOELECTRIC APPLICATIONS

Scientific adviser:
Dr. Măriuca Gartner

PhD Student:
Mariana Balaban (married Chelu)

Bucharest, 2021

Summary

1.	**INTRODUCTION**	**3**
2	**LITERATURE REVIEW ON OXIDIC MATERIALS**	**6**
2.1.	**SnO_2-based thin film and nanostructures**	**6**
2.2.	**ZnO-based thin film and nanostructures**	**7**
2.3	**General considerations on film and oxidic nanostructures synthesis**	**10**
2.4	**Preparation methods of nanostructured oxidic materials**	**11**
2.5	**Sol-gel method**	**11**
2.6	**Microwave assisted sol-gel method**	**13**
2.7	**Hydrothermal method**	**14**
2.8	**Nucleation and particle growth theory**	**15**
2.9	**Chemical sensors – general characteristics**	**18**
2.10	**SnO_2 thin films based electrochemical sensors**	**19**
2.11	**Gas sensors – general characteristics**	**23**
2.12	**Piezoelectric materials – general characteristic**	**28**
3.	**OBJECTIVES OF THE THESIS**	**33**
4.	**MATERIAL CHARACTERIZATION TECHNIQUES**	**34**
EXPERIMENTAL RESULTS		**37**
5.	**Materials with electroanalytic properties**	**38**
5.1.	**Electrodes modified with tin oxide films**	**38**
5.2.	**Structural characterization**	**40**
5.3.	**Morphological characterisation**	**41**
5.4.	**Electrochemical characterisation**	**44**
5.5.	**Electrochemical detection of nitrite**	**47**
5.5.1.	**Voltametric determination of nitrite**	**51**
5.5.2.	**Amperometric determination of nitrite**	**52**
5.6.	**Partial results**	**56**
6.	**Materials with gas detection properties**	**58**
6.1.	**ZnO-NiO based nanostructured materials**	**59**
6.2.	**Substrate description**	**59**
6.3.	**Chemical synthesis**	**60**

6.4. Structural characterization 61
6.5. Morphological characterisation 62
6.6. Formaldehyde detection properties 64
6.7. Partial results 67
7. Materials with piezoelectric properties 68
7.1. PMMA/ZNO 1D nanostructures deposited on metallic substrate (Pt, Au, Ti) 70
7.1.1. Obtaining ZnO films by sol gel method 72
7.1.2. Obtaining 1D ZnO nanostructures by hydrothermal synthesis 73
7.1.3. Polymers used in piezoelectric applications 74
7.1.4. Ellipsometric measurements 76
7.1.5. Structural characterization 77
7.1.6. Morphological characterization 81
7.1.7. Piezoelectric measurements 89
7.1.8. Electrical measurements 93
7.2. PMMA / CuO / ZnO / Pt nanostructures 98
7.2.1. Structural characterisation 100
7.2.2. Morphological characterisation by SEM 101
7.2.3. Piezoelectric measurements 103
7.3. ZnO nanostructures doped with Li or Ag 104
7.3.1. Structural characterisation 106
7.3.2. Morphological characterisation by AFM 109
7.3.3. Partial conclusions 125
8. General conclusions, original contributions, future research, dissemination 126
8.1. General conclusions 126
8.2. Original contribution 129
8.3. Future research 130
8.4. Dissemination 131

Note: Page numbering in this table of contents corresponds to the doctoral thesis.

Keywords: sensors, piezoelectric properties, sol gel, nanostructures

Introduction

As the understanding of nanometric materials evolves, the importance of obtaining them with active surfaces that are as large as possible is also growing, which ensures a high sensitivity for technological applications in sensoristic, environmental or medical field [1-9]. Materials such as SnO_2 and ZnO that are abundant in nature and non-toxic are studied from the perspective of new approaches, due to their excellent chemical capacities and stability [10 - 15].

The main objective of the thesis is the **synthesis and realization of nanostructured oxide materials by sustainable and environmentally friendly methods**, **for sensors and piezoelectric applications** that make the transfer from the laboratory stage to the technological level.

The **design** strategy considers the modeling, selection and combination of precursors and optimal synthesis methods, suitable for the substrates used.

The thesis presents the results obtained on the synthesis and testing of three nanomaterial systems: **SnO_2, ZnO-NiO**, as well as nanostructures of **ZnO 1D, CuO-ZnO** and **ZnO 1D doped with Li or Ag.**

(1) For **SnO_2**, a complex investigation was performed regarding the formation of modified electrodes with oxide thin films, but also for obtaining an electrochemical sensor. The sensor was obtained from solutions prepared by the microwave-assisted sol gel and sol gel method and integrated in an electrochemical platform that makes it possible to use it as a mobile mini-device.

(2) For the **ZnO-NiO** system, 1 D type microstructures were made in several stages, using both the sol gel method and the hydrothermal technique. Microstructures obtained by combining very simple and inexpensive synthesis methods are a way to improve the classic gas detection materials, by increasing the active surfaces and selectivity.

(3) For **non-doped ZnO** and **Li or Ag doped ZnO systems**, **1 D type nanostructures** were made and for **CuO-ZnO** nanostructures of "nano-flowers" type were obtained. By combining the sol gel deposition method with the hydrothermal one, together with the use of polymers with special characteristics, such as **PMMA** (polymethylmethacrylate) or **PVDF** (polyvinylidene fluoride) these materials showed piezoelectric properties

Different substrates were used for each of these three material systems.

The design of the nanostructured materials was made according to the configuration, dimensions, material and type of substrate used for each system. The entire design of sensing film and piezo active components (nanostructured materials deposited on substrates) has been developed considering with final applications in mind.

This thesis is structured in 8 chapters that aim to achieve the proposed objectives.

In **Chapter 1**, Introduction, after a brief presentation of the importance of the approached field, the main purpose of the thesis is highlighted.

Chapter 2 contains general information on the importance of nanostructured oxide materials such as SnO_2 and ZnO, which together with other semiconductor oxides can lead to

the production of sensors or components for power generation. The basic notions regarding both chemical sensors and piezo-active materials, their applications, the detection mechanisms involved in the sensory process, as well as the energy generation mechanisms were specified.

Chapter 3 highlights the main objective of the thesis, as well as the specific objectives

Chapter 4 is dedicated to the presentation of methods for characterizing oxide nanomaterials from a structural, morphological, electrical, electroanalytical and piezoelectric point of view.

The experimental results of the doctoral thesis are presented in chapters 5-7, as follows:

Chapter 5 presents the results on obtaining, characterizing and testing materials with electrocatalytic properties based on SnO_2 films, as well as developing an electrochemical sensor and integrating it into an electrochemical platform for the detection of nitrite ions in running water.

Chapter 6 presents the study of a microsensor that contains a sensing film based on ZnO-NiO dedicated to the detection of gases, such as volatile organic compounds. The possibility of obtaining a microsensor with low energy consumption, leading to the environmental detection of formaldehyde according to the standard conditions of a commercial gas sensor, was investigated.

Chapter 7 is dedicated to the study of materials with piezoelectric properties deposited by chemical methods in several steps on multiple complex substrates, leading to energy generation. Three systems of materials were made: 1D ZnO coated with polymethylmethacrylate (PMMA), CuO-ZnO coated with PMMA and 1D ZnO doped with (Li, Ag) coated with polyvinylidene fluoride (PVDF).

Chapter 8 presents a summary of the most important contributions made by this thesis, as well as the dissemination of results.

Materials with electroanalytical properties

In this chapter the results obtained following a complex study on obtaining, characterizing and optimizing new electrodes (Figure 1) modified with SnO_2 films deposited on electrochemical transducers for the detection of nitrogen species in water are presented.

Consequently,

- modified electrodes were prepared with SnO_2 films, synthesized both by the classical sol gel method (abbreviated C) and by the microwave-assisted method (abbreviated MW);

- the obtained electrodes were characterized by electrochemical and physico-chemical methods;

- an electrochemical sensor was developed for the detection of nitrite ions in running water.

The crystalline structure of the thin films (deposited from solutions synthesized by the classical sol gel method and the microwave-assisted one) obtained after heat treatment was characterized by X-ray diffraction (Figure 2). For both types of deposits, two crystalline phases of cassiterite were identified.

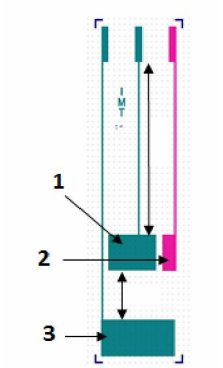

Figure 1 Electrochemical structure with 3 electrodes on Pt /Ti /SiO_2 /Si substrate; 1-working electrode; 2-reference electrode; 3-auxiliary electrode

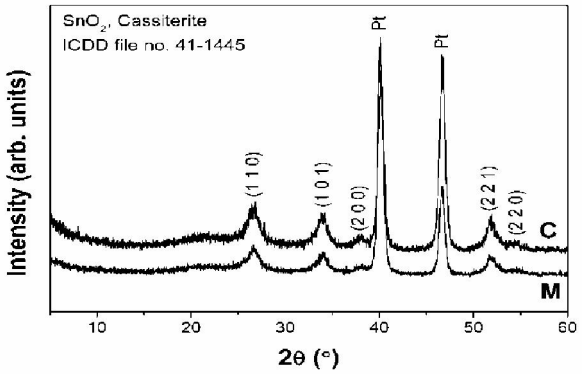

Figure 2 X-ray diffractograms of SnO_2 thin films prepared by the classical method (C) or by the microwave-assisted method (MW)

The morphology of both types of films investigated by AFM measurements showed a specific porosity of the SnO_2 sol gel film, induced by the preparation method (Figure 3). SEM images showed SnO_2 coatings showing nongranulated surfaces (Figure 4).

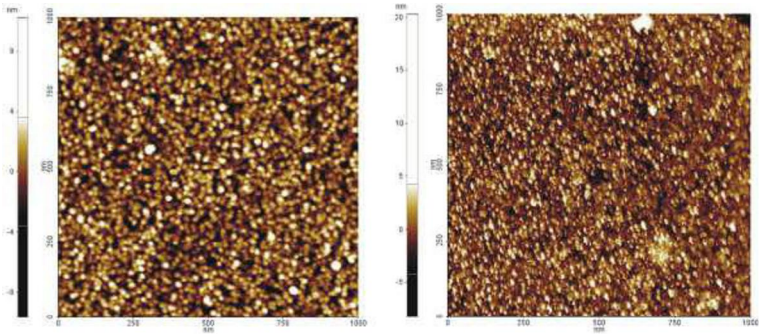

Figure 3 2D AFM images of the SnO_2 films deposited on the working electrode, by sol-gel method (left) and microwave assisted sol-gel method (right) together with representative line-scans, along the red lines

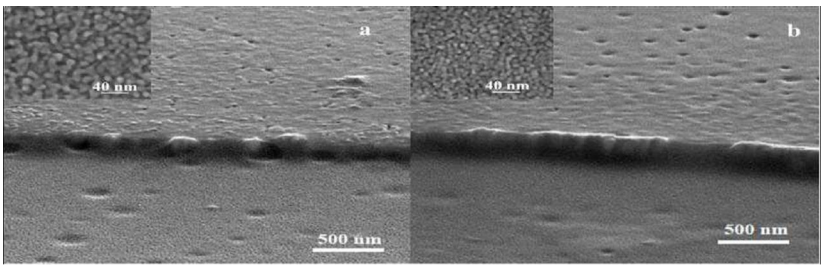

Figure 4 SEM micrographs for SnO2 films prepared by classic sol-gel (a) and MW assisted sol gel

Both types of films were electrochemically characterized by cyclic voltammetry and electrochemical impedance spectroscopy (Figures 5, 6).

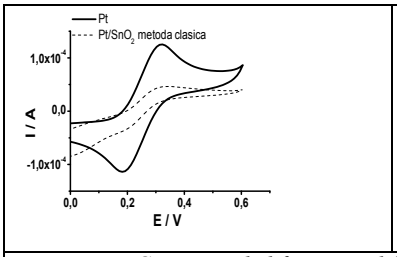

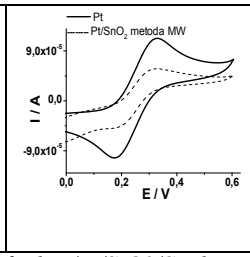

Figure 5 CVs recorded for unmodified Pt/Ti/SiO2/Si electrode and modified Pt/Ti/SiO2/Si with SnO2 coating prepared by classic sol gel method (a) and MW assisted method (b)

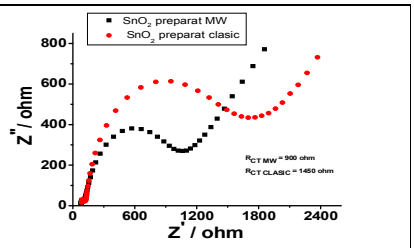

Figure 6 EIS spectra (Nyquist diagrams) for the SnO2 films prepared by classic sol gel and MW assisted method in 0.5 M KNO3 containing 5 mM K4 [Fe(CN)6] / K3 [Fe(CN)6]

The areas of electroactive surfaces for SnO_2 films obtained by both methods were calculated using the Randles-Sevcik equation:

$$Ip = 2{,}69\ x\ 10^5 A\ D^{\frac{1}{2}}\ n^{\frac{3}{2}}\ v^{\frac{1}{2}}\ C, \qquad (1)$$

Where n is the number of electrons involved in the redox process, A is the electrode area (cm^2), D is the diffusion coefficient of the species in solution (7.6 × 10–6 $cm^2\ s^{-1}$), C is the concentration of the species in the solution volume (mol cm^{-3}) and v is the scanning speed of the potential (V s^{-1}). The electroactive surfaces of SnO_2 films prepared by classical methods assisted by sol gel and MW were 0.024 and 0.032 cm^2. There is an increase of approximately 33% of the electroactive surface for SnO_2 coating prepared by the MW assisted method compared to that obtained by the classical sol gel method.

Considering all the results obtained from the morphological, structural and electrochemical characterizations for the two types of coatings, the following investigations were performed only for SnO_2 films obtained by the microwave-assisted method because these results suggested better conductivity and electron transfer capacity.

For the electrochemical oxidation of nitrite ions to nitrate ions, the number of electrons transferred to the interface between the electrode and the electrolyte solution was calculated, according to the **Laviron equation:**

$$Ip = \frac{nFQv}{4RT} \qquad (2)$$

where, Q is the consumed charge obtained by integrating the area of the anodic peak, Ip the anodic peak current for nitrogen, n the number of electrons consumed, v the scanning speed, F the Faraday constant, R the gas constant and T the temperature.

The peak current increased with the scanning speed according to the equation:

$$Ip\ (A) = 4{,}9 \times 10^{-5} + 5{,}28 \times 10^{-4}\ v\ (Vs^{-1}) \qquad (3)$$

The number of electrons involved in the general reaction was 2, and the electrochemical oxidation of nitrite ions at the electrode interface at the SnO_2/Pt/Ti/SiO_2/Si electrode with the electrolyte solution could be considered a two-electron transfer reaction.

The proposed mechanism for NO_2^- oxidation could be expressed using the following reactions:

$$2\,NO_2^- \leftrightarrow 2\,NO_2 + 2e^- \quad (4)$$

$$2NO_2 + H_2O \leftrightarrow 2H^+ + NO_2^- + NO_3^- \quad (5)$$

From the study of the sweep rate on the oxidation process of nitrite ions it was concluded that this is a process controlled by both diffusion and surface (adsorption of species on the surface), the current increased linearly with both the square root of the sweep rate and the velocity sweeping.

The study of the effect of the pH of the buffer solution on the response of the electrochemical sensor showed that the pH equal to 5 is the optimal one for the detection of nitrite ions (Figure 7). The peak oxidation current increased from pH 3 to pH 5 and decreased to pH values greater than 5.

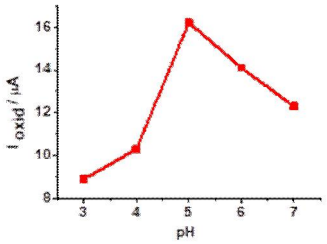

Figure 7 Oxidation current versus pH for SnO_2/Pt/Ti/SiO_2/Si electrode in 0.1 M PBS containing 0.8 mM NO_2^-

Therefore, the 0.1 M phosphate buffer solution with pH = 5 was chosen as the electrolyte for all electrochemical measurements.

SnO_2 films prepared by MW-assisted sol gel method showed excellent electrocatalytic activity in oxidation of nitrite ions.

According to the Drinking Water Directive (Council Directive 98/83 / EC of 3 November 1998), the maximum permissible limit on nitrogen in water is 0.5 mg/l. The sensor response prepared by the MW-assisted sol gel method was tested by chronoamperometry. Successive additions of different concentrations of nitrite ions were made in the 0.1 M PB solution of pH = 5, at an applied potential of 0.8V. Figure 8 shows the amperometric response of the SnO_2/Pt/Ti/SiO_2/Si electrode during the addition of different concentrations of nitrite ions. During this time, the 0.1M PB solution was stirred continuously at a constant speed. A rapid electrode response was demonstrated by the fact that the current signal increased rapidly when a certain concentration of nitrite ions was added and the response current reached a steady state for less than 3 seconds.

The electrochemical sensor developed based on SnO_2 films showed a linear response both on the concentration range between 0.01 and 0.4 mM and on the concentration range between 0.4 and 1 mM. The calibration curve with the error bar of the electrode modified with SnO_2 film is inserted in Figure 8, and the corresponding equation is:

$$I\,(\mu A) = 0{,}16 + 22{,}56\,C\,(mM) \quad (6)$$

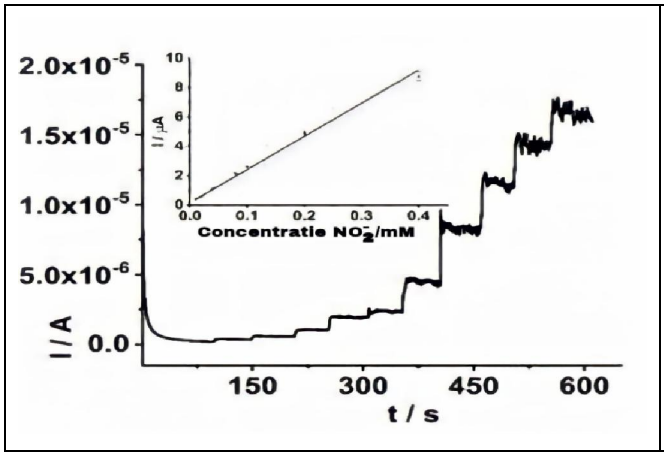

Figure 8 Chronoamperogram recorded at SnO_2/Pt/Ti/SiO_2/Si electrode in 0.1 M PBS, pH=5 containing 0.01, 0.02, 0.04, 0.08, 0.1, 0.2, 0.4, 0.6, 0.8 and 1mM NO_2^-

In the linear range 0.01 to 0.4 mM, the sensitivity obtained was 22.56 μA / mM and the limit of detection (LOD) was 1.7 (± 0.05) μM (0.08 mg / L, less than the EC directive limit of 0.5 mg/L). The limit of quantification (LOQ) was 5.6 (± 0.16) μM (0.27 mg / l).

Selectivity and recovery studies in real samples

The electrochemical sensor response prepared using the MW-assisted sol gel method (SnO_2/Pt/Ti/SiO_2/Si) was not influenced by any of the interfering species used in the present study (Figure 9), the current remaining unchanged until the next addition of nitrite ions when the signal increased. The concentration of interfering species (like KNO_3, Na_2SO_4, $CaCl_2$, Na_2CO_3, KCl and glucose) was five times higher (1 mM) than the concentration of nitrite ions (0.2 mM).

The next step in the development of the electrochemical sensor was to establish the degree of recovery in real samples such as: milk (Dorna), beer (Ursus), mineral water (Bucovina) and water from the regional distribution network. The samples were diluted (1: 9) with 0.1 M phosphate buffer, pH = 5 to which a known concentration of nitrite ions was added. The degree of recovery in water samples was between 100 and 110%, and for beer and milk was 83.3 and 90%. This response demonstrates a good performance of the sensor, its response not being influenced by the matrix effect of the sample.

The response of the developed sensor was tested after four weeks, during which time the analytical signal decreased by 20%, demonstrating an acceptable operational stability.

The detection limit of the electrochemical sensor was 1.7 μM (0.08 mg / L), concentration below the limit of the European directive (0.5 mg / L).

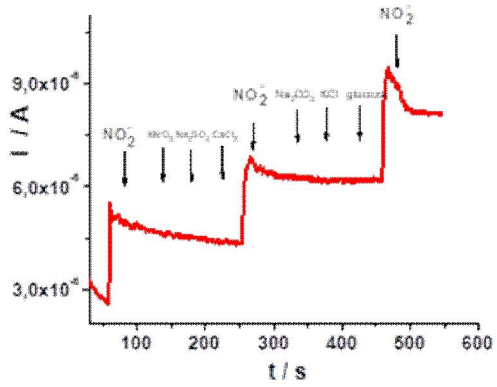

Figure 9 Amperometric response at SnO_2/Pt/Ti/SiO_2/Si modified electrode toward nitrite ions in the presence of interfering species as KNO_3, Na_2SO_4, $CaCl_2$, Na_2CO_3, KCl, and glucose

The results showed that:

- New electrodes modified with SnO_2 films were prepared to determine nitrite ions in water. SnO_2 films were prepared by the microwave-assisted sol gel and sol gel method and deposited dropwise on the working electrode surface. Uniform and stable coatings were obtained.

- In comparison, SnO_2 films prepared by the microwave-assisted sol gel method displayed higher electrochemically active surface characteristics. The morphological and structural characterization highlights that the films show a good crystallinity and uniformity, as well as the formation of smaller particles in the SnO_2 film prepared by the sol gel method irradiated in the microwave field, compared to the SnO_2 film obtained by the classical sol gel method, with a less uniform distribution, which can lead to an increase in reactivity.
- The SnO_2 films obtained were stable and showed very good electrocatalytic properties in the oxidation of nitrite ions.

- The response of the electrochemical sensor for nitrite detection was linear on concentration range from 10 to 400 µM, with a sensitivity of 22.56 µA / mM and a detection limit of 1.7 µM (0.08 mg/L). This sensor presented a good degree of recovery in real samples and a good selectivity in the presence of possible interfering species.

- The method used for the preparation of modified electrodes is affordable, cheap and easy to make.

- The SnO_2 Pt/Ti/SiO_2/Si sensor has been integrated in an electrochemical platform that can function as a portable mini-device for the detection of nitrite ions in water. This platform has 4 tanks in which water samples are introduced for the detection of the pollutants.

Materials with gas sensing properties

This chapter presents the results of the study on obtaining, characterizing and testing of ZnO / NiO microstructures for the detection of the gaseous formaldehyde. The following were considered:

- Obtaining through chemical synthesis of ZnO/NiO bi-component films, using simple methods, by liquid exfoliation and hydrothermal synthesis (sau growth);

- Morphological and structural caracterisation of the obtained microstructure;

- Testing of the gas sensing properties of volatile organic compounds, in particular of formaldehyde.

The ZnO/NiO sample was deposited on miniaturized alumina (transducers) substrates, with Au interdigitated electrodes on the frontside and a Pt heater on the backside (*Figure 10*).

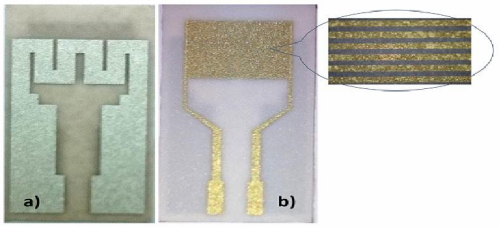

Figure 10 Alumina transducer with:

a) Pt heater on the back side, b) Au interdigitated electrode (IDE) on the front side

The sensitive layer was obtained by a simple, inexpensive and environmentally friendly chemical approach, by increasing hierarchical ZnO structures on NiO nanoparticles, by liquid exfoliation and hydrothermal synthesis.

In the first step, a NiO layer was deposited. This was obtained by liquid exfoliation and thermal treatment at 350 ^{o}C for 1 hour, with a heating rate of 5 ^{o}C / min.

The second step was the growth of ZnO microstructures by hydrothermal synthesis on the thin layer of sintered NiO granules, to obtain ZnO/NiO sensing films. The sensor was heat treated at 350 ^{o}C for 1 hour, with a heating rate of 5 ^{o}C / min.

In the X-ray spectra (Figure 11) for the obtained sample, in addition to the substrate reflections (Au and alumina), the presence of NiO (maximum intensity line) was detected, as well as the zincite phase of zinc oxide, with a pronounced preferential orientation according to the direction [001]. The morphological characterization performed by AFM highlighted the presence of the NiO layer deposited on the Au / alumina substrate (Figure 12).

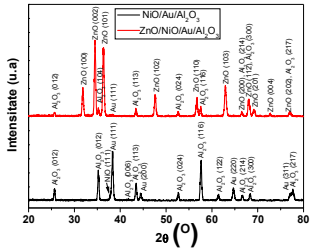

Figure 11 XRD for NiO / Au / alumina and ZnO / NiO / Au / alumina

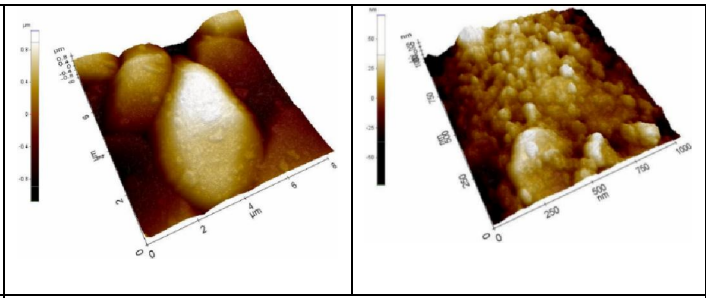

Figure 12 AFM 3D images NiO/Au/alumina

The ZnO layer deposited over the NiO / Au / alumina film was recorded at the scale of (8x8) μm^2 due to the large rods (a few microns in length) developed during the hydrothermal synthesis (Figure 13). ZnO microstructures (MS) grown hydrothermally are strongly attached and hierarchical formed on the NiO layer surface as micro-blocks, randomly oriented on the surface. From Figure 13 we can see that the ZnO / NiO microstructure obtained is very

orderly, continuous and uniform and has well-aligned massive blocks (most probably composed of adjacent ZnO rods, column type) with lengths of a few microns. The appearance of the sample suggests that the thickness of the hydrothermal increased ZnO film is large enough not to highlight the substrate granules. The analyzed microstructures play an important role in increasing the active detection surface of the sensitive film.

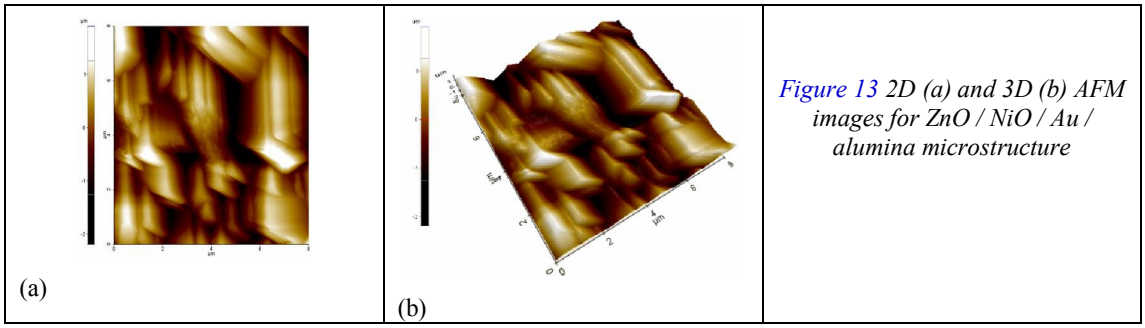

Figure 13 2D (a) and 3D (b) AFM images for ZnO / NiO / Au / alumina microstructure

The electrical response of the realized microstructure, in the presence of different concentrations of formaldehyde, at room temperature, is presented in Figure 14.

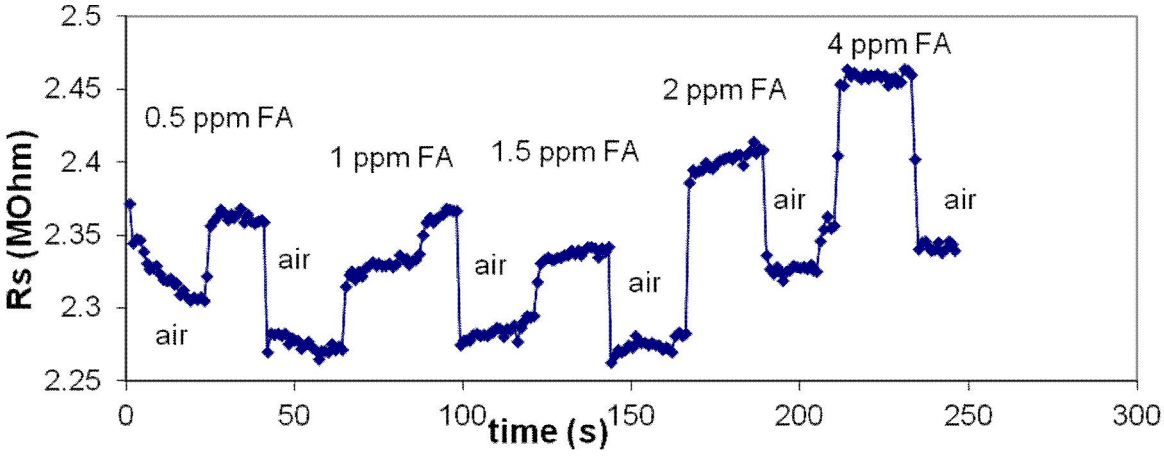

Figure 14 Sample response for different concentrations of formaldehyde, Tcam, DC

Obtained results:

• Fabrication of a n-p type microstructure ZnO / NiO deposited on a miniaturized transducer with Au / alumina layer, by chemical syntheses from the solution.

• The NiO layer was synthesized by liquid exfoliation, and the ZnO microstructure was grown on the NiO layer by hydrothermal synthesis at low temperature.

• XRD analysis revealed the presence of the zincite phase of ZnO.

• AFM images highlighted the formation of a well-aligned micro-blocks type ZnO microstructure, deposited over a granular NiO layer.

• ZnO / NiO sensing films showed formaldehyde detection sensitivity at room temperature, with a detection limit of 0.5 ppm.

• The sample was obtained by a simple, easy method, at low temperature and from non-toxic precursors.

Materials with piezoelectric properties

This chapter presents the experimental results on the design, synthesis by chemical methods, characterization by different techniques and testing of piezoelectric materials, obtained by a "green" chemical approach. 1D materials that have a direct piezoelectric effect can be used in the development of sustainable energy generation and storage devices. *Obtaining unconventional energy, by converting mechanical energy into a source of electricity, with intelligent, biocompatible materials and by cheap methods is a topical direction for the energy field and for the environment.*

In this thesis, the influence of the substrate on the structural, morphological and piezoelectric characteristics was investigated by comparative study of 1D ZnO nanostructures deposited on rigid metallic substrates such as **Pt**/Ti/SiO_2/Si and **Au**/Ti/SiO_2/Si and on flexible metallic substrate, such as **Ti** foil. **Pt** or **Au**/Ti/SiO_2/Si type metal substrates were dimensionally designed for piezoelectric applications and manufactured within IMT Bucharest.

Using these three different metal substrates, three piezoelectric structures of ZnO 1D type, were obtained under similar synthesis conditions. Using these three different metal substrates, three piezoelectric structures of ZnO 1D type, were made under similar synthesis conditions.

The main factors influencing the quality of the seed layer and their nucleation were studied: the concentration of the solution, the thickness of the seed layer and the heat treatment.

Three piezoelectric models were obtained:

• PMMA / ZnO nanowires deposited on Pt, Au or Ti substrates,

• PMMA / CuO / ZnO nanostructures deposited on Pt substrate

• PVDF / ZnO nanowires doped with (Li or Ag) deposited on Pt or Ti substrates.

1. **1D PMMA / ZnO nanostructures deposited on metallic substrates (Pt, Au, Ti)**

These materials were obtained by chemical synthesis in several stages.

The thickness of the ZnO seed layer was determined by ellipsometric measurements. Thus, for the layer deposited on Pt/Ti/SiO_2/Si the thickness of the layer was about 60 nm, and for the layer deposited on Ti foil the thickness was about 90 nm.

The structural characterization highlighted the presence of the zincite phase of ZnO, with a wurtzite structure (Figure 15). It was observed that all samples showed a dominant diffraction line for the plane (002), which indicates a high degree of anisotropic growth of ZnO nanowires along the c-axis or direction [001]. The mean crystallite size was calculated to be ~ 21 nm for the samples without polymer and ~ 25 nm for the samples with polymer.

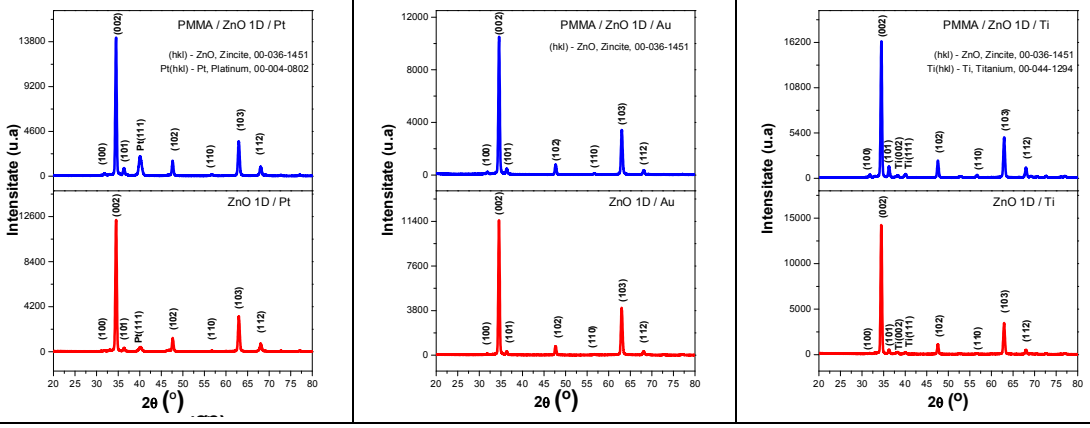

a b c

Figure 15 XRD for 1D ZnO and PMMA/ZnO 1D deposited onto substrate :

a) Pt/Ti/SiO_2/Si ; b) **Au**/Ti/SiO_2/Si; c) Ti foil

The morphology of the structures deposited on the Au/Ti/SiO_2/Si substrate was investigated by TEM (Figures 16-19) and SEM (Figures 20-21).

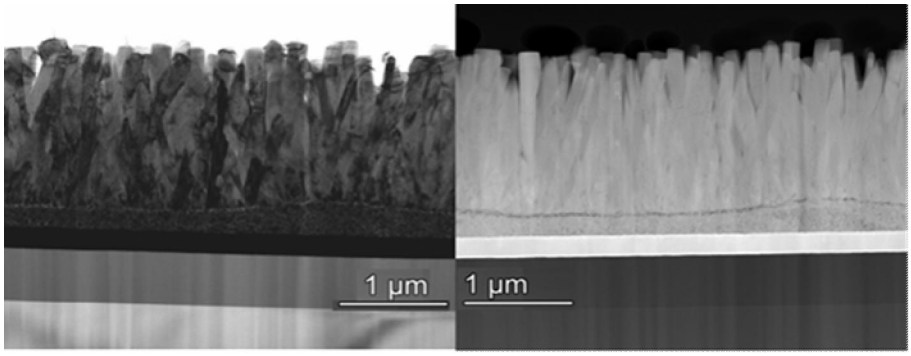

Figure 16 BF TEM and HAADF images from ZnO 1D sample coated with PMMA on Au

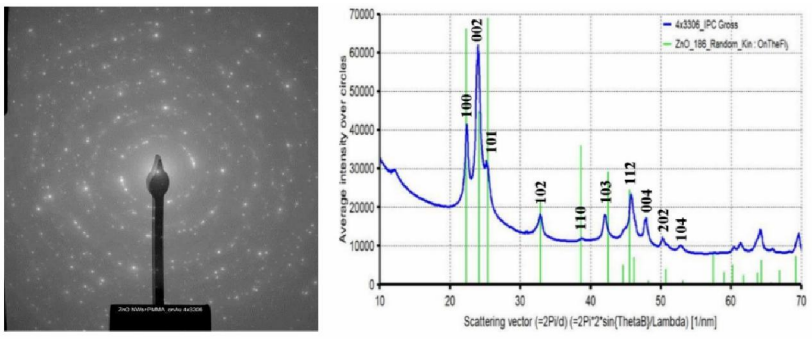

Figure 17 SAED 2D pattern (left) and 2θ integrated intensity figure (right), from the ZnO layer in the ZnO 1D + PMMA on Au sample.

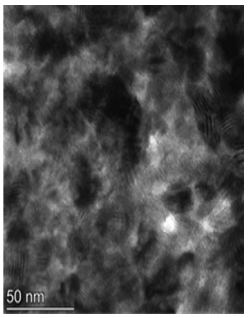

Figure 18 HRTEM image from the nanocrystalline ZnO seed layer between the gold layer and the columnar ZnO layer.

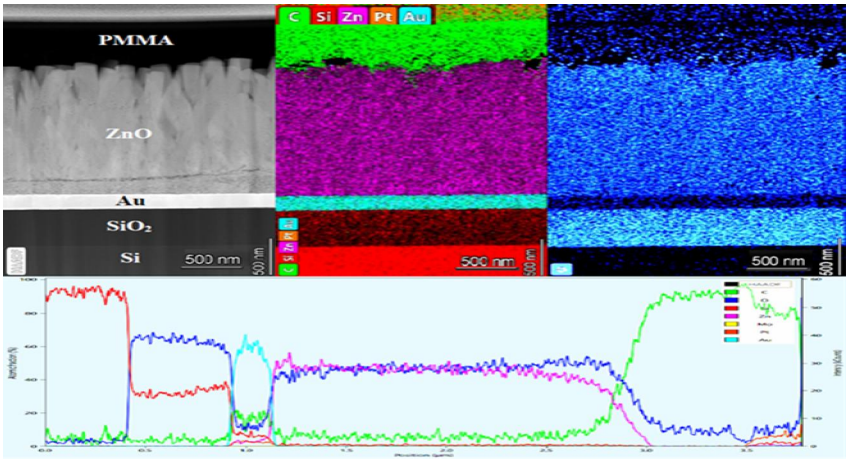

Figure 19 *HAADF and EDS map: C-green, Si-red, Zn-magenta, Au-cyan (center) and O-blue (right) from the PMMA-coated ZnO 1D+PMMA on Au sample*

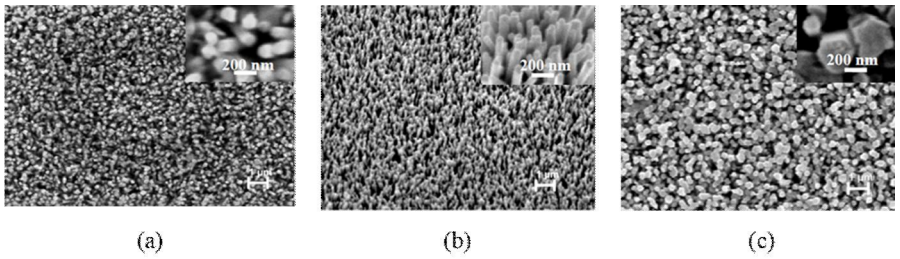

Figure 20 *Top view SEM micrographs of well-aligned ZnO 1D before PMMA deposition grown onto different metallic substrates: (a) Pt; (b) Au; (c) Ti*

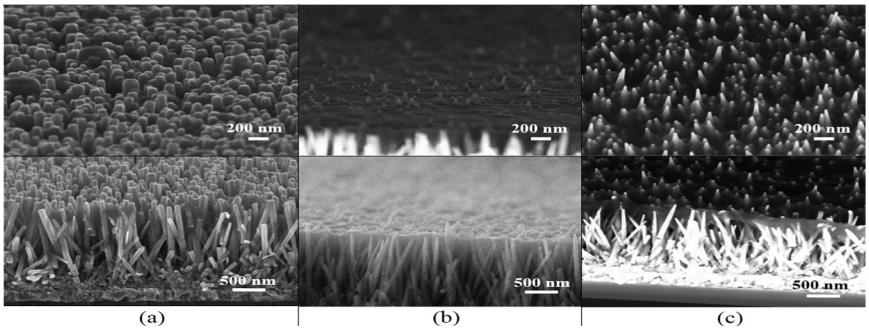

Figure 21 *Edge view- SEM micrographs of ZnO NWs after PMMA deposition grown onto: (a) Pt substrate; (b) Au substrate; and (c) Ti substrate*

The piezoelectric structures were made by silver metallization on the face for the Ti foil, and for the Pt and Au substrates both on the front and on the back of the samples. The testing of the piezoelectric properties was done by measuring the direct piezoelectric coefficient d_{33} (Figures 22-23).

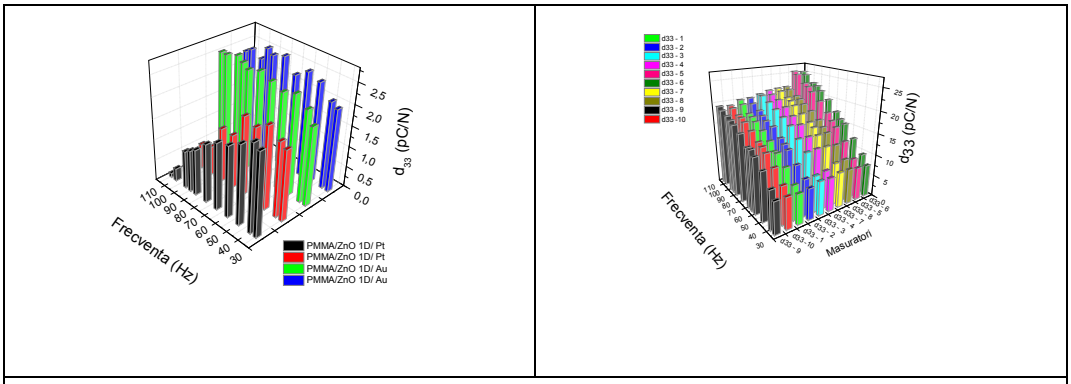

a b

Figure 22 Plot of frequency as a function of piezoelectric coefficient d_{33} for samples: a) PMMA/ZnO 1D on Pt and Au and c) on Ti foil, in the 30 - 110 Hz domain

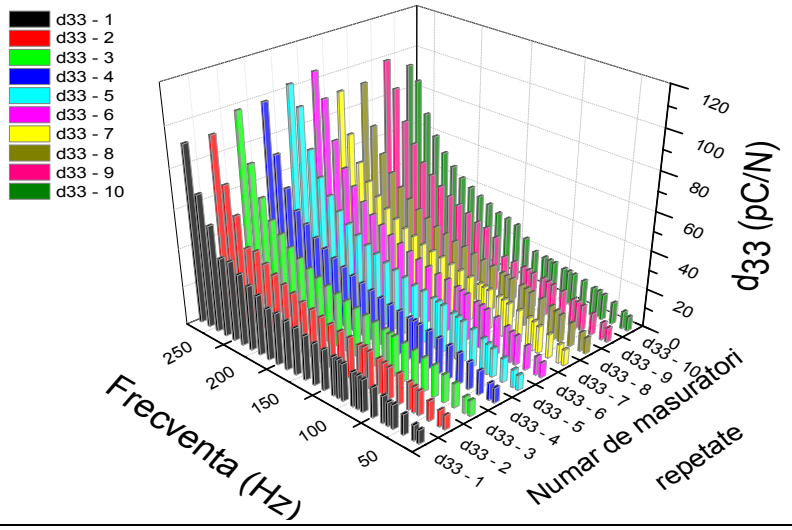

Figure 23 Graphical representation of the frequency dependence of the piezoelectric coefficient d_{33} for the PMMA / ZnO 1D / Ti sample on the frequency range between 30 and 250 Hz

To optimize the 1D PMMA / ZnO piezoelectric structures deposited on the Pt substrate, the speed and the spinning time of the sol gel solutions were varied, to obtain the ZnO seed layer, as well as the thickness of the polymer layer. Electrical measurements were performed for the optimized samples in direct current, using an external upper electrode, by varying the static pressing force. Various values of the output voltage, the resistances of the two samples were recorded (as an average of three recorded values) and the intensity, current density and power density were calculated, depending on the area of each sample. The measurement of the electrical properties for the PMMA / ZnO 1D sample performed on Ti foil which showed the best piezoelectric performance, was performed by impedance spectroscopy. This measurement provided additional information about the relationship between the piezoelectric performance of the device and its relationship to the structure and mechanism of energy conversion (Figure 24).

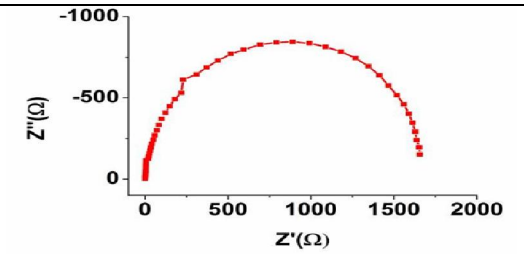

Figure 24 Nyquist representation for PMMA/ZnO 1D /Ti showing real and imaginary components of impedance (Z) measured between 100 Hz and 2 MHz.

2. PMMA / CuO / ZnO / Pt nanostructures

This piezoelectric model was obtained by a four-step synthesis, following the steps described in the previous chapter for the structure of PMMA / ZnO 1D / (Pt, Au, Ti). The difference was in the third stage, when CuO nanostructures were obtained by hydrothermal synthesis at low temperature. The PMMA / CuO / ZnO / Pt nanostructure was obtained (Figure 25), which was characterized by XRD (Figure 26) and SEM (Figure 27), then the direct piezoelectric coefficient d33 was measured over a frequency range between 30 and 110 Hz (Figure 28).

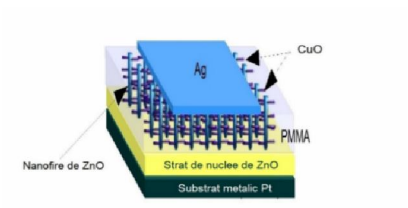

Figure 25 Graphical representation of the steps for obtaining the PMMA / CuO / ZnO / Pt structure

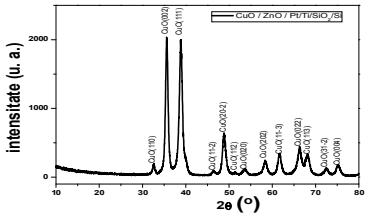

Figure 26 X-ray diffractogram for CuO / ZnO / Pt sample

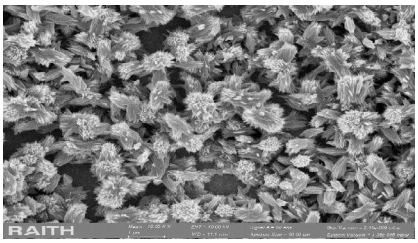

a

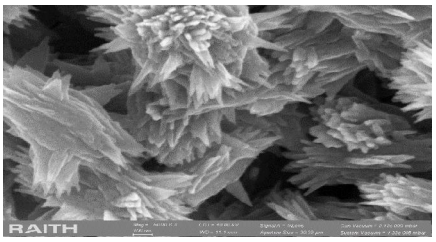

b

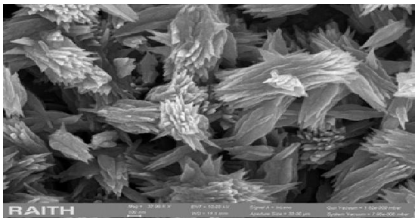

c

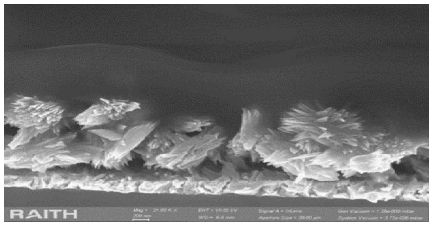

d

Figure 27 High magnification SEM images for CuO/ZnO/Pt sample uncovered (a, b, c) and coated with PMMA (d)

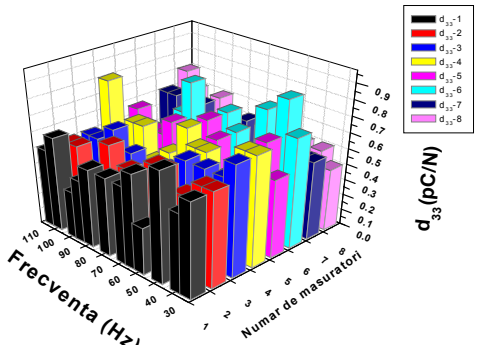

Figure 28 Graphical representation of the piezoelectric coefficient as a function of frequency

3. ZnO nanostructures doped with (Li or Ag)

The ZnO nanostructures doped with Li or Ag were made following the same steps of chemical synthesis from the solution presented to obtain non-doped ZnO nanowires. The metallic substrates used for the realization of these models were Pt/Ti/SiO_2/Si and Ti foil. The obtained structures were assembled in polymeric matrices from polyvinylidene fluoride solution (PVDF) and were characterized structurally and morphologically by AFM (Figures 29-32) and SEM (Figures 33-35).

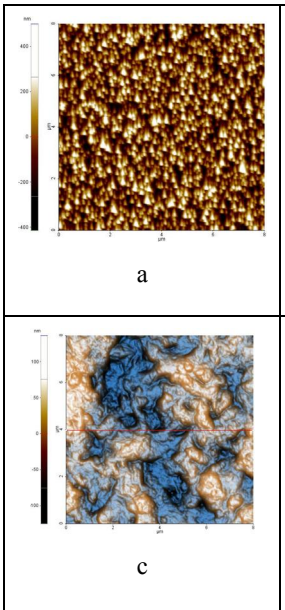

Figure 29 2D (a) and 3D (b) AFM images for ZnO sample doped with Li (HT) uncovered (a, b) and coated with PVDF (c, d) deposited on Pt

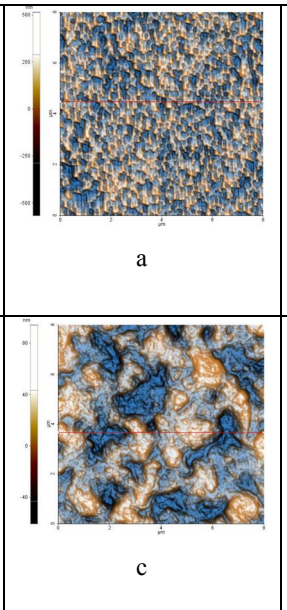

Figure 30 AFM images for ZnO sample doped with Li (HT) uncovered (a, b) and coated with PVDF (c, d) deposited on Ti

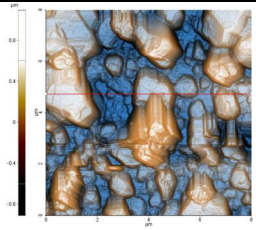

a

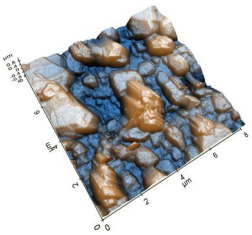

b

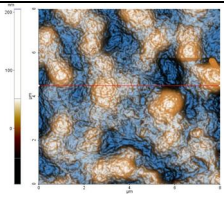

c

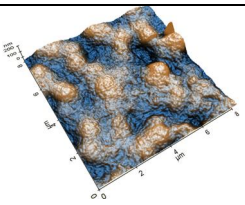

d

Figure 31 2D (a) and 3D (b) AFM images for ZnO sample doped with Ag (HT) uncovered (a, b) and coated with PVDF (c, d) deposited on Pt

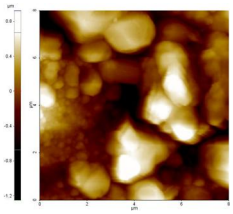

a

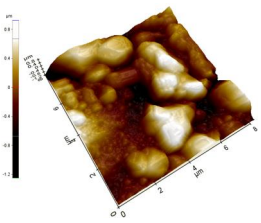

b

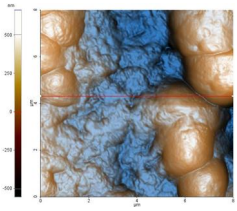

c

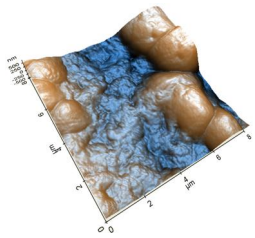

d

Figure 32 AFM images for ZnO sample doped with Ag (HT) uncovered (a, b) and coated with PVDF (c, d) deposited on Ti

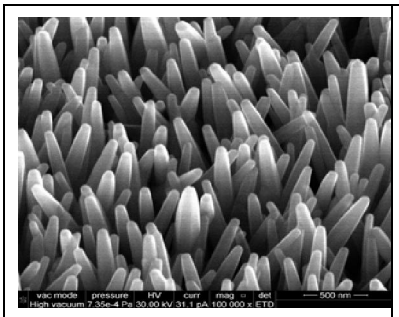

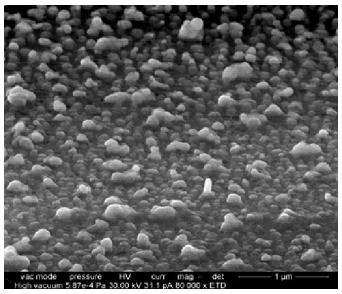

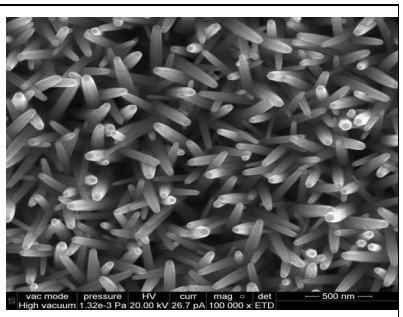

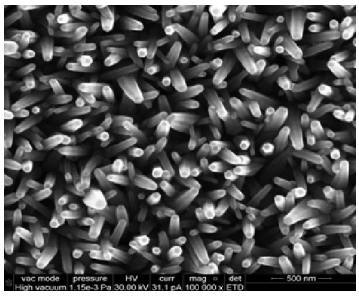

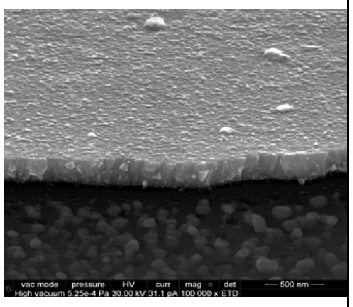

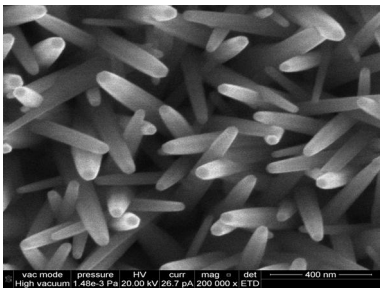

Figure 33 SEM images for Li-doped ZnO sample deposited on Pt substrate

Figure 34 SEM images for Ag-doped ZnO sample deposited on Pt substrate

Figure 35 SEM images for the Li-doped ZnO sample deposited on the Ti substrate

The piezoelectric properties of (Li, Ag) doped 1D ZnO materials were tested by measuring the piezoelectric coefficient d_{33} (Figure 36). The best answer was given by the PVDF / Ag-ZnO sample deposited on the Pt substrate.

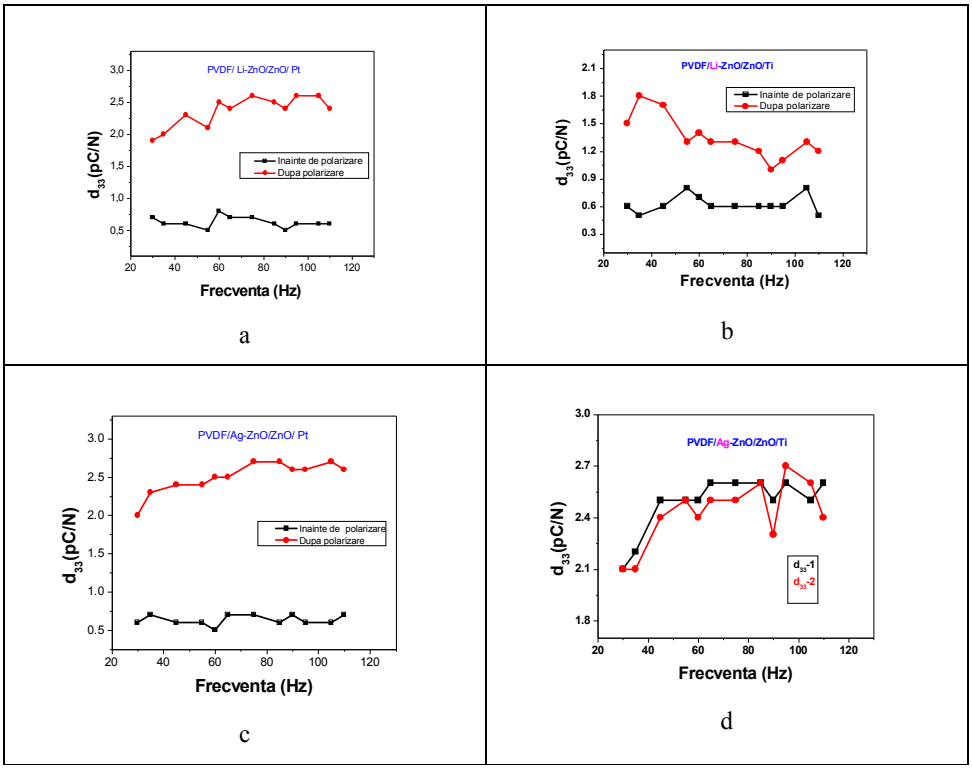

Figure 36 Frequency dependence of the piezoelectric coefficient for PVDF / ZnO doped with Li / Pt (a), PVDF / ZnO doped with Li / Ti (b), PVDF / ZnO doped with Ag / Pt and PVDF / ZnO doped with Ag / Ti (d)

The results led to the following conclusions:

- In this chapter, three types of piezoelectric nanostructures were obtained: ZnO 1D, CuO / ZnO and ZnO 1D doped with (Li, Ag), on rigid metallic substrates of multilayer type (Pt and Au) and flexible of the foil type Ti, coated with PMMA or PVDF polymers.

- For the first type, XRD investigations confirmed the development of a hexagonal crystal structure. For the second type, the presence of the tenorite phase of CuO was found. For the third type, the network parameters showed that the Ag doping ion replaced the Zn centers in the crystalline matrix of the nanowires, and the Li doping ion that replaces the Zn ions was incorporated into the ZnO network.

- AFM measurements showed large hemispherical cavities, up to 2 μm in diameter and up to 750 nm in depth for PMMA coating in the case of the first model. For the doped 1D ZnO model, uniform deposits of the ZnO core layer for all substrates were highlighted. In the case of the dopant ion Li, a uniform growth of nanowires was observed, and in the case of Ag a non-uniform growth on all substrates. PVDF coating was uniform for all samples, with small differences due to the influence of the substrate.

- The electrical measurements performed in direct current showed low output values for the measured samples, compared to other PZT or AlN type materials, but stable and comparable to the values of ZnO-based structures in the literature.

- By impedance spectroscopy, using a simple RC model, the internal resistance for the 1D PMMA / ZnO sample deposited on Ti, (1.2 kΩ) was approximated and the internal capacity was calculated (12.51 nF).

- All nanostructures showed piezoelectric properties. The comparative results showed that for the samples deposited on rigid metallic substrates coefficients of 2-3 pC / N are obtained, and for the samples deposited on flexible substrate, the coefficient d_{33} is between 6.9 and 112 pC/N.

General conclusions

In this thesis, studies were carried out grouped on three research directions stated in the introduction:

1. Materials with electroanalytical properties

- Using the classical sol gel method and the microwave-assisted sol gel method, modified electrodes were obtained with **SnO_2 films** deposited on electrochemical transducers.

- By choosing and optimizing the deposition parameters and the heat treatment, uniform and stable coatings were obtained. In comparison, SnO_2 thin films made from microwave assisted sol-gel method showed a larger electrochemically active surface.

- It was observed that the microwave irradiation of sol gel solutions led to the obtaining of films with uniform and stable surface having electroanalytical properties, for the detection of nitrite ions in water.

- An electrochemical sensor for selective nitrite detection was obtained, which showed a linear response over a concentration range between 10 to 400 μM, with a sensitivity of 22,56 μM / mM and a limit of detection of 1,7 μM, as well as the good degree of recovery in real samples and a good selectivity in the presence of interference.

- The obtained sensor was integrated in an electrochemical platform, as a portable mini-device, for applications of detection of nitrite ions from natural waters (Figure 37).

2. Materials with gas detection properties

- **ZnO / NiO microstructures** deposited on microtransducers were obtained, by combined methods of liquid exfoliation and hydrothermal synthesis, simple and environmentally friendly ways.

- The microstructures were characterized structurally and morphologically and were investigated for the detection of gaseous formaldehyde. The morphology of the nanostructured sample showed a large active surface, which was correlated with the detection properties.

- The success of these microtransducers consists in the detection of formaldehyde (0.5 ppm) at room temperature, a goal pursued with priority in recent years, leading to energy savings.

3. Materials with piezoelectric properties

- A method of obtaining materials with piezoelectric architectures using non-toxic materials has been developed, through hydrothermal synthesis reactions at low temperatures.

- Three models of piezoelectric materials, coated with different polymers (PMMA and PVDF), were prepared on simple metal substrates of flexible type, or multilayer, of rigid type:

a) **1D PMMA / ZnO** deposited on Pt /Ti/SiO_2/Si, Au/Ti/SiO_2/Si or Ti substrates,

b) **PMMA / CuO / ZnO** deposited on Pt/Ti/SiO_2/Si substrates ;

c) **1D PVDF / ZnO doped with (Li or Ag)** deposited on Pt/Ti/SiO_2/Si or Ti substrates.

- The obtained models were characterized structurally, morphologically, ellipsometrically, electrically and piezoelectrically. Ellipsometric measurements revealed the thickness of the seed layer deposited between the substrate and the nanowire layer of ZnO increased in the next step.

- The complex morphological investigation highlighted the 1D type structure of zinc oxide or "nano flowers" type.

- The piezoelectric performances were evaluated comparatively for the models made, both from a morphological point of view, by measuring the direct piezoelectric coefficient, d_{33}.

- The electrical properties of the obtained nanostructures were investigated, by measuring the direct output currents.

- The best piezoelectric response was obtained for the **ZnO nanostructure** with **1D morphology coated with PMMA** and deposited on **Ti** in the range of 6.9 - 112 pC / N, for a frequency range between 30 and 250 Hz (Figure 38).

Figure 37 Electrochemical detection platform developed:(1) Sample container, (2) detection device, (3) lid, (4) 3D printed media

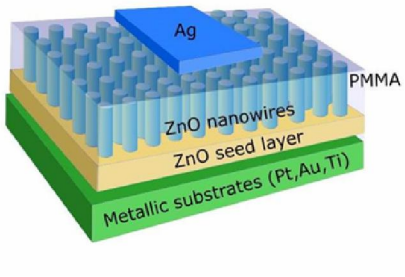

Figure 38 Schematic representation of the piezo-active structure obtained

Original contributions

Considering the original results obtained in this doctoral thesis and reporting on the current knowledge in the field of chemical sensors and piezoelectric materials, the contributions of this thesis are the following:

- Development of an electrochemical sensor for the detection of nitrogen based on sol-gel films of SnO_2, which has been integrated into an electrochemical platform that functions as a portable mini-device for the detection of nitrite ions in running water.

- Obtaining a microsensor based on ZnO / NiO bi-component sensing films, with formaldehyde detection properties at room temperature, which will be integrated in a portable device;

- Design of multilayer materials, consisting of a 1D ZnO structure coated with polymers that led to a material with a very high piezoelectric coefficient in case of deposition on flexible metal substrate of Ti.

Future research directions

The studies undertaken in this thesis pave the way for new directions of development of:

- Piezoelectric materials in the direction of practical biomedical applications, by deepening and optimizing the systems based on ZnO made, but also the development of other systems of materials, as well as their characterization and testing.

- Integration of piezoelectric systems in devices that generate "green energy".

- Development of stable and reproducible materials as sensors for greenhouse gases (CH_4, CO_2, O_3).

- Obtaining new biomaterials by synthesis methods of the "green" chemistry, which can be integrated as sensors

Selective references

[1] M. O. Orlandi, Tin oxide materials. Elsevier Inc., 2020.
[2] K. Aguir et al., Trends in metal oxide thin films: Synthesis and applications of tin oxide. Elsevier Inc., 2020.
[3] A. Janotti and C. G. Van De Walle, "Fundamentals of zinc oxide as a semiconductor," Reports Prog. Phys., vol. 72, no. 12, 2009.
[4] G. V. Aguilar, "Introductory Chapter: A Brief Semblance of the Sol-Gel Method in Research," in Sol-Gel Method-Design and Synthesis of New Materials with Interesting Physical, Chemical and Biological Properties, IntechOpen, 2018.
[5] D. Nunes et al., Synthesis, design, and morphology of metal oxide nanostructures'', 2019.
[6] G. Cao, "Nanostructures and Nanomaterials: Synthesis, Properties and Applications." World Scientific, 2004.
[7] X.-Y. Yu et al., "Nanostructured metal oxides/hydroxides-based electrochemical sensor for monitoring environmental micropollutants," Trends Environ. Anal. Chem., vol. 3–4, pp. 28–35, 2014.
[8] A. Mirzaei et al., "Resistive gas sensors based on metal-oxide nanowires," J. Appl. Phys., vol. 126, no. 24, 2019.
[9] J. Briscoe and S. Dunn, "Piezoelectric nanogenerators - a review of nanostructured piezoelectric energy harvesters," Nano Energy, vol. 14, pp. 15–29, 2014.
[10] I. Dakua and N. Afzulpurkar, "Piezoelectric energy generation and harvesting at the nano-scale: Materials and devices," Nanomater. Nanotechnol., vol. 3, no. 1, 2013.
[11] C. Lete et al., "Nitrite electrochemical sensing platform based on tin oxide films," Sensors Actuators, B Chem., vol. 316, no. November 2019, p. 128102, 2020.
[12] M. Chelu et al., "High-quality PMMA/ZnO NWs piezoelectric coating on rigid and flexible metallic substrates," Appl. Surf. Sci., vol. 529, no. February, p. 147135, 2020.
[13] M. H. Malakooti et al., "Enhanced energy harvesting through nanowire based functionally graded interfaces," Nano Energy, vol. 52, pp. 171–182, 2018.
[14] J. Briscoe et al., "Measurement techniques for piezoelectric nanogenerators," Energy Environ. Sci., vol. 6, no. 10, pp. 3035–3045, 2013.
[15] G. Romano et al., "Piezoelectric potential in vertically aligned nanowires for high output nanogenerators," Nanotechnology, vol. 22, no. 46, 2011.

[16] S. Dey et al., “Voltage-controlled NiO/ZnO p–n heterojunction diode: a new approach towards selective VOC sensing,” Microsystems Nanoeng., vol. 6, no. 1, pp. 1–9, 2020.